Journal of Applied Mechanics and Technical Physics, Vol. 35, No. 5, 1994

BEHAVIOR OF SUSPENSIONS UNDER DYNAMIC LOADING

S. V. Stebnovskii

UDC 532.135:532.528

A homogeneous newtonian liquid having a shearing-stress relaxation time λ_0 of about 10^{-10}-10^{-8} sec is an almost ideally fluid medium; it does not retain shearing stresses at realistic strain rates (the St. Venant limiting stress is zero for it). On the other hand, a solid has λ_0 of hours or even much longer times, i.e., shows viscoelastic behavior for arbitrarily low shearing strain rates.

Although there is a vast amount of information on solid failure mechanics [1], research on the failure dynamics of homogeneous liquids has begun only quite recently. On sufficiently rapid stretching, a liquid develops cavitation, which is accompanied by the formation of discontinuities [2-4], which resemble cracks in a solid. This has been used in research on the macrorheological characteristics of a cavitating stretched liquid [5-7], where it has been shown that $\lambda_0(\alpha_0)$ increases with the volume concentration of cavitation bubbles α_0, and that such a liquid acquires viscoelastic behavior. However, the properties vary continuously as α_0 increases, which greatly complicates researching the failure mechanism.

Dynamic failure is of interest, particularly for a medium that in the equilibrium state has macrorheological characteristics intermediate between those of a homogeneous newtonian liquid and a solid (information on failure in such media is needed to construct a general model for dynamic failure in condensed media, which include liquids and solids).

Here I show that emulsions and suspensions in the equilibrium state have characteristics intermediate between newtonian liquids and solids, so their behavior on pulsed loading is important in this respect.

1. Dependence of the rheological characteristics on disperse-phase concentration. According to [[8], the effective viscosity μ' is dependent on the volume concentration of the droplets α_1 in the emulsion as follows:

$$\bar{\mu}' = \frac{\mu'(\alpha_1)}{\mu'(\alpha_1 = 0)} = \left[1 + \frac{0.8415\alpha_1/(\alpha_1)_{\bar{\mu}'=100}}{1 - 0.8415\alpha_1/(\alpha_1)_{\bar{\mu}'=100}}\right]^{2.5}, \tag{1.1}$$

in which $(\alpha_1)_{\bar{\mu}'=100}$ is the volume concentration of droplets corresponding to $\bar{\mu}' = 100$.

Consider a dispersed-solid suspension for low values of the volume concentration of solid particles α_2, where the effective viscosity μ'' is independent of the strain rate $\dot{\varepsilon}$ but increases with α_2, which is closely described by the Mooney equation [9]

$$\bar{\mu}'' = \mu''(\alpha_2)/\mu''(\alpha_2 = 0) = \exp[k_0\alpha_2/(1 - \alpha_2/\alpha_{2*})]. \tag{1.2}$$

Here $k_0 = 2.5$ for rigid spherical particles, while α_{2*} is the maximum volume concentration of the particles for the closest packing ($\alpha_{2*} = 0.74$-0.77). However, μ'' increases rapidly with α_2 above 0.35, and (1.2) does not correspond to the process, since the medium acquires the state of a non-newtonian liquid and for $\alpha_2 \to \alpha_{2*}$ loses its mobility and goes over to the bound state. As $\dot{\varepsilon}$ increases, the μ_*'' decreases, which corresponds to α_{2*}, on account of reorientation of the unsymmetrical particles, disruption of the aggregates, and other factors.

For characteristic shearing-strain times $\Delta\tilde{t}$ much less than the shearing-stress relaxation time λ_0, a liquid behaves as an elastic body of rubber type. Therefore, for an emulsion with $\Delta\tilde{t} << \lambda_0$, one can neglect the difference in the elastic moduli for shearing in a liquid matrix $G_{1\infty}$ and the liquid dispersed phase $G_{2\infty}$, and the medium can be considered as a continuous solid having the dynamic shear elastic modulus $G_\infty' \simeq G_{1\infty}$. Then from (1.1) we have the relation for the shear-stress relaxation time in an emulsion:

Novosibirsk. Translated from Prikladnaya Mekhanika i Tekhnicheskaya Fizika, No. 5, pp. 68-77, September-October, 1994. Original article submitted December 14, 1993; revision submitted March 10, 1994.

0021-8944/94/3505-0704$12.50

$$\lambda'(\alpha_1) \simeq \lambda_0 \left[1 + \frac{0.8415\alpha_1/(\alpha_1)_{\bar{\mu}'=100}}{1 - 0.8415\alpha_1/(\alpha_1)_{\bar{\mu}'=100}} \right]^{2.5}. \tag{1.3}$$

Then as the bulk concentration of droplets increases, so does this relaxation time in an emulsion, which acquires viscoelastic behavior. The elastic energy in such a medium accumulation during shearing on account of droplet deformation, i.e., increase in surface energy.

For $\Delta\tilde{t} << \lambda_0$, a suspension can also be represented as an elastic rubber-type body, but filled with more rigid particles of corresponding shape. Then the expression for the elastic modulus [9] gives

$$\frac{G''_\infty}{G_{1\infty}} = \frac{1 + (k_0 - 1)B\alpha_2}{1 - B[1 + (1 - \alpha_{2*})\alpha_2/\alpha_{2*}^2]\alpha_2}, \tag{1.4}$$

in which $B = (G_{2\infty}/G_{1\infty} - 1)/[G_{2\infty}/G_{1\infty} + (k_0 - 1)]$, G_∞'' being the shearing modulus of the suspension; $k_0 = 2.5$ for rigid spherical particles, and $G_{2\infty}$ is the dynamic shear modulus of the particle material. As $G_{1\infty}/G_{2\infty} \leq 1$, we have on the basis that $k_0 = 2.5$

$$B = \frac{1 - G_{1\infty}/G_{2\infty}}{1 + \frac{3}{2}\frac{G_{1\infty}}{G_{2\infty}}} = 1 - \frac{5}{2}\frac{G_{2\infty}}{G_{1\infty}} + \ldots,$$

and consequently we get from (1.4) that

$$G''_\infty \simeq G_{1\infty}\left\{ \frac{1 - \frac{3}{2}\left(1 - \frac{5}{2}\frac{G_{1\infty}}{G_{2\infty}}\right)\alpha_2}{1 - \left[1 + \left(\frac{1 - \alpha_{2*}}{\alpha_{2*}^2}\right)\alpha_2\right]\left(1 - \frac{5}{2}\frac{G_{1\infty}}{G_{2\infty}}\right)\alpha_2} \right\}. \tag{1.5}$$

Then we use (1.2) and (1.5) to get the shearing-stress relaxation time in a suspension as

$$\lambda''(\alpha_2) = \frac{\mu''}{G''_\infty} = \lambda_0 \frac{\left\{1 - \left[1 + \left(\frac{1 - \alpha_{2*}}{\alpha_{2*}^2}\right)\alpha_2\right]\left(1 - \frac{5}{2}\frac{G_{1\infty}}{G_{2\infty}}\right)\alpha_2\right\}\exp\left(\frac{5\alpha_2/2}{1 - \alpha_2/\alpha_{2*}}\right)}{1 + \frac{3}{2}\left(1 - \frac{5}{2}\frac{G_{1\infty}}{G_{2\infty}}\right)\alpha_2}, \tag{1.6}$$

which implies that $\lambda''(\alpha_2)$ increases with α_2 as that quantity goes from 0 to α_{2*}, and for $\Delta\tilde{t} << \lambda''$, the system will accumulate elastic energy. However, energy accumulation in a suspension can occur only on account of the elastic strain energy in the solid particles. If the particles are virtually incompressible, i.e., $G_{2\infty} \to \infty$, (1.5) implies that for low and medium α_2

$$G''_\infty\big|_{G_{2\infty}\to\infty} \simeq G_{1\infty}\frac{1 - 3\alpha_2/2}{1 - \left[1 + \left(\frac{1 - \alpha_{2*}}{\alpha_{2*}^2}\right)\alpha_2\right]\alpha_2}$$

and correspondingly form (1.6)

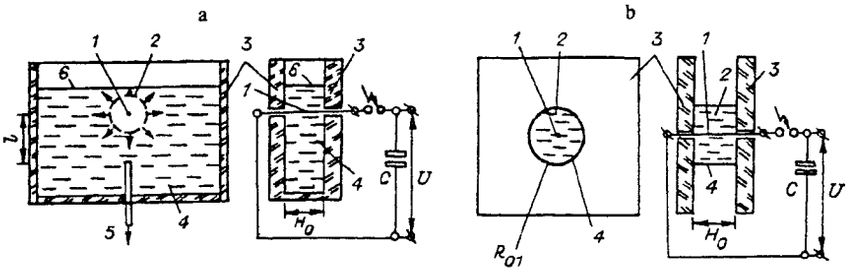

Fig. 1

$$\lambda'' \big|_{G_{2\infty}\to\infty} \simeq \lambda_0 \frac{\left\{1 - \left[1 + \frac{(1-\alpha_{2*})}{\alpha_{2*}^2}\alpha_2\right]\alpha_2\right\}}{1 + 3\alpha_2/2} \exp\left[\frac{3}{2}\alpha_2/(1 - \alpha_2/\alpha_{2*})\right]. \tag{1.7}$$

However, the increase in μ'' is bounded as α_2 increases, since μ'' decreases as $\dot{\varepsilon}$ increases [9], and

$$\lambda'' = \frac{\mu''}{G''_\infty} \to 0 \text{ for } G_{2\infty} \to \infty,\ \alpha_2 \to \alpha_{2*},$$

i.e., the elastic stresses in shear strain relax almost instantaneously in a highly concentrated suspension of undeformable particles, and only viscous stresses are present, which are dependent on the strain rate.

Emulsions and suspensions thus take an intermediate position in the rheological series between newtonian liquids and solids, so research on the failure dynamics is important.

2. I have examined by experiment the behavior of restricted volumes (specimens) of emulsions and suspensions in shock-wave loading followed by stretching in the unloading wave. The emulsion consisted of drops of I-20 machine oil (size 0.05-0.6 cm) in an aqueous alcoholic solution having a volume concentration of droplets $\alpha_1 \approx 0.3$; that medium is denoted by C1.

I also examined three types of suspension: sand with particle size 30-100 μm and $\alpha_2 \simeq 0.65$-0.7 (α_2 close to α_{2*}) in water (medium C2); spherical elastic particles of divinylbenzene–styrene copolymer (density $\rho_1 = 1.05$-1.08 g/cm^3, particle size 50-500 μm) suspended in water with added glycerol to equalize the densities of the dispersed phase and matrix and having volume particle concentration $\alpha_2 \simeq 0.35$ (medium C3); and one with the same composition but having $\alpha_2 \simeq 0.65$ (medium C4).

The shock loading was provided by exploding a thin manganic wire 1 (type PMM, diameter 0.02 cm, Fig. 1a, b) having length H = 3 cm by the discharge of a bank of high-voltage capacitors (C = 1 μF, U = 17 kV). The experiments were performed in two ways: 1) generating a cylindrical shock wave 2 (Fig. 1a) in a planar tank (50 × 40 × 3 cm) having parallel transparent walls 3 and filled with the medium 4; 2) shock loading by exploding the wire 1 (Fig. 1b) in a cylindrical volume of medium 2 having radius R_{01} and bounded by the transparent plane-parallel plexiglas walls 3 and the thin paper readily-broken cylindrical shell 4. In the first state, the shock-wave parameters were measured with the pressure sensor 5 (Fig. 1a) placed at various distances l from the wire axis.

An SFR-1 high-speed camera recorded the flow at the stretching stage after reflection of the cylindrical shock wave from the planar free surface 6 (Fig. 1a) in the first state and from the cylindrical free surface 4 (Fig. 1b) in the second state, which was placed in a plane perpendicular to the wire axis.

3. The following result were obtained. The series of experiments with cylindrical waves showed that the damping rate for a given α_1 (or correspondingly α_2) was dependent on the ratio of the acoustic impedance of the matrix material z_1 and the dispersed phase z_2 for an emulsion:

$$k' = \frac{z_1}{z_2} = \left(\frac{\rho_1}{\rho_2}\frac{K_1}{K_2}\right)^{1/2} \tag{3.1}$$

while for a suspension

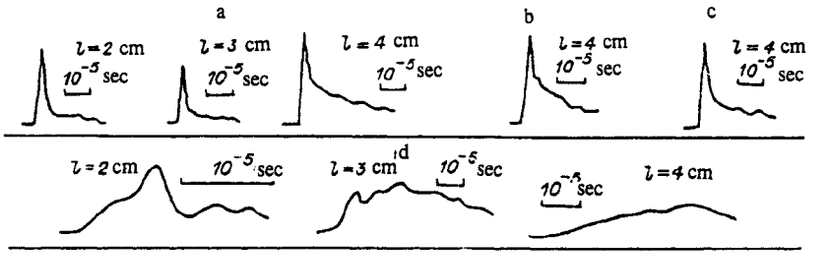

Fig. 2

$$k'' = \frac{z_1}{z_2} = \left[\frac{\rho_1 K_1}{\rho_2\left(K_2 + \frac{4}{3}G_2\right)}\right]^{1/2}, \tag{3.2}$$

in which K_1, K_2, and G_2 are the fulk and shear elastic moduli.

Figure 2 shows typical pressure waveforms. Here a are the test waveforms in pure water (wave amplitude $P_0 = 3.4 \cdot 10^7$ $l = 2$ cm, $P_0 = 3.1 \cdot 10^7$ Pa for $l = 3$ cm, and $P_0 = 2.7 \cdot 10^7$ Pa for $l = 4$ cm); b represents the Cl medium with $l = 4$ cm and shows the ratio of the wave amplitude $P_*(l = 4$ cm) namely $P_* = P_*/P_0 \approx 1$; c is for medium C4 with $l = 4$ cm, where $P_* = 0.9$; and d is for C2 where $P_* = 0.09$ for $l = 2$ cm, $P_* = 0.04$ for $l = 3$ cm, and $P_* = 0.03$ for $l = 4$ cm (in the last case, the amplitude attenuation and the profile evolution agreed well with the [11] data).

From (3.1) and (3.2), C1, C3, C4 and C2 $k_{C1}' \approx 1 > k'' = k_{C3}" = k_{C4} = 0.78 > k_{C2}" = 0.012$ for the four media, and $P_*(l = 4$ cm) $|_{C1} \approx 1 > P_*(l = 4$ cm) $|_{C4} = 0.9 > P_*(l = 4$ cm) $|_{C2} = 0.013$ correspondingly, i.e., the less k, the more rapid the damping. As k' and k"are determined by the ratios of the elastic moduli of matrix and dispersed phase, one can assume that at least one of the main reason for the damping in a highly concentrated suspension is that the energy is dissipated at the particles because of the difference in compressibility between the liquid matrix and the particles.

The compression-wave damping is dependent also on the particle concentration,but here the wave processes are considered only for highly concentrated suspensions and only to the extent that they given an indication of the wave parameters and the tension in the medium arising at the unloading stage.

High-speed recording of emulsion Cl behind the compression front and in the unloading zone showed as follows. The drops, even of the largest size (0.4-0.6 cm), remained undisrupted after interaction with the shock wave: the emulsion is an essentially transparent medium for the compression wave. In the unloading stage, cavitational bubbles arise at the interfaces and in the drops and fragment the medium. At the loading rates and energies used in these experiments, the process does not differ qualitatively from cavitational failure in a homogeneous liquid [5-7, 12]. Special research is needed to determine the quantitative characteristics.

Figure 3 shows typical recordings of the structure evolution in a suspension due to stretching in the unloading zone after reflection from the free surface. Here a is the loading state in accordance with Fig. 1a, with h = 1 cm the distance from the wire to the free surface in medium C2, where the solid particles were lyophilic, i.e., wetted by the liquid; b represents also Fig. 1a with h = 1 cm and a test medium consisting of dry sand at the poured density, i.e., a difference form C2 was there here the gaps between the particles were filled by air, and in such a medium there is no connectedness apart from the elasticity of the air; c shows loading as in Fig. 1b, where $R_{01}(0) = 2$ cm with medium C4, and where the solid particles were lyophobic, i.e., not wetted by the liquid.

Parts a and b of Fig. 3 show that the liquid component in C2 produces connectedness because of the wetting, and this results in cellular structures in the unloading stage, in contrast to the air-sand medium (Fig. 3a, frames 3 and 4). The cells are formed because pores grow in the stretched suspension.

Figure 3a shows that the volume of the dome 1 is greater than that of the explosion cavity 2 at the corresponding stage, and since the dispersed phase and matrix are incompressible, it can be explained only by the growth of pores (the mode of formation and growth is not considered here). However, pore growth should [6] reduce the dynamic shear modulus, and thus increase the shear relaxation time. When the medium is stretched, the sand particles remain almost unperformed, and (1.7) shows that $\lambda"$ is close to λ_0 for low and medium α_2, while $\lambda" \to 0$ for $\alpha_2 \to \alpha_{2*}\alpha" \to 0$. Then as the pore concentration α_0

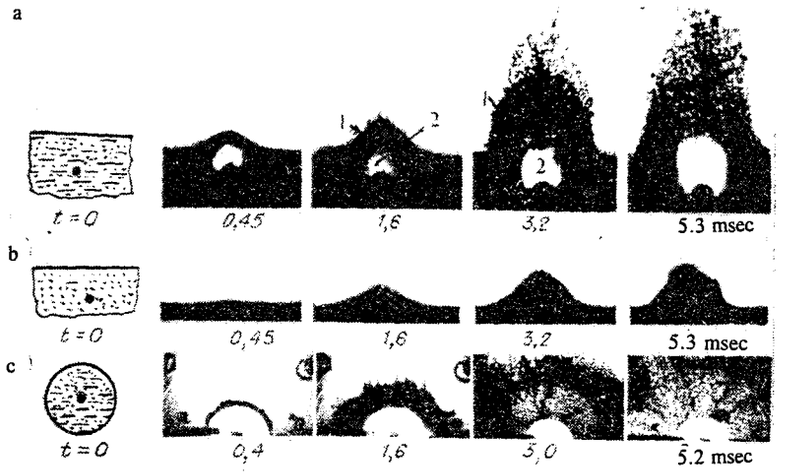

Fig. 3

increases in medium C2, the compressibility should increase, i.e., G_∞" is reduced at least without reducing μ". Consequently, $\lambda" = \mu"/G_\infty"$ in C2 should increase with α_0.

It is extremely difficult to determine the α_0 dependence of $\lambda"$, and this requires detailed experiments on the morphology evolution in a three-phase medium at various stretching rates.

There is extensive shock-wave energy dissipation when C2 is loaded, so discontinuities are not formed during the unloading stage because of the low stretching rate: disruption occurs only because the pores are transformed to cells (Fig. 3a) followed by capillary break-up in the links between them. The links consist of liquid matrix containing solid particles in the bound state on account of the wetting forces.

The [13] method shows that after the dome 1 has broken up (Fig. 3a), there is a flow of droplet-type fragments consisting of solid particles bound by the liquid, as shown in Fig. 4a, which shows a photograph of imprints from the fragments on the immersion layer (1 is the outer boundary of an imprint from the liquid component of a fragment and 2 those from the solid particles present in it). If a fragment during flight breaks up into smaller elements, they also consist of particles linked by liquid. A lyophilic suspension thus has stable structure: the fragments formed after disruption retain the features of the lyophilic suspension.

The radial stretching for the cylindrical volume of C4 in the unloading zone (Fig. 3c) shows that the volume increases during the stretching because pores develop, which in that case are probably of cavitational origin, and cellular structures are formed by their unlimited growth (Fig. 3c, frames 3 and 4). However, a difference from C2 is that C4 produces separation between the fractions: lyophobic particles are injected from the liquid matrix into the atmosphere in such a way that the thin links between cells contain virtually none of them.

The fragmentation of C4 results in escaping liquid droplets containing hardly any particles together with a flux of lyophobic particles, as is evident from the histogram (Fig. 4b) constructed by the method described in [13]. Here nl is the number of fragments in the flow having suspension features, namely consisting of solid particles and liquid matrix, while n2 is the number of pure droplets, and n3 the number of solid particles.

4. We explain the structure formation in the fragments by considering the condition for thermodynamic stability of the suspension structure in relation to the lyophilicity, and also to the volume and number concentrations. We assume that the particles are frozen into the liquid matrix.

We compared the levels of the free energy F′ for system 1 (Fig. 5a) consisting of a suspension fragment containing a liquid matrix (1) and solid particles (2) and also of the surrounding air shell (0) with the energy level F" of system 2 (Fig. 5b) to which system 1 (subsequently s1) goes over when the structure becomes unstable: separation of the liquid and solid phases. The isothermal transition of s1 to system 2 (subsequently s2) is produced only by capillary and inertial forces. The dashed lines indicate the boundaries of the systems, including the air shells, which are such that the total volumes of the systems coincide Here S_1 is the free surface of s1, which contains N spherical particles (for convenience) equal in size, while S_1' is

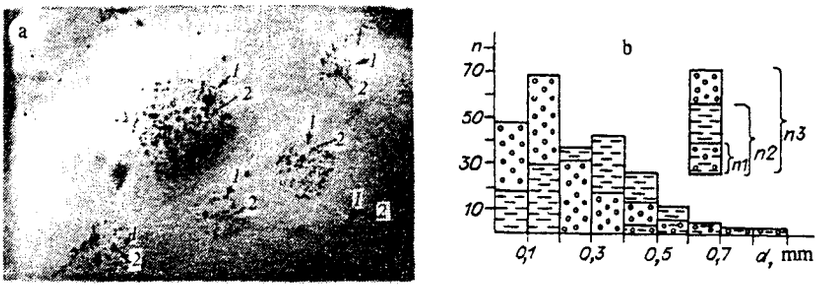

Fig. 4

the free surface of the liquid volume from which all the particles in the air shell have been removed (Fig. 5b), S_2 is the surface of a solid particles, and σ_{10}, σ_{12}, and σ_{20} are the interfacial tensions at the liquid-air, liquid-solid, and solid-air boundaries respectively.

Then the difference between the levels of the total free energy for s1

$$F' = \rho_0 V_0 F_0 + \rho_1 V_1 F_1 + \rho_2 V_2 F_2 + \sigma_{10} S_1 + \sigma_{12} S_2 N \tag{4.1}$$

and s2

$$F'' = \rho_0 V_0 F_0 + \rho_1 V_1 F_1 + \rho_2 V_2 F_2 + \sigma_{10} S_1' + \sigma_{20} S_2 N \tag{4.2}$$

is put as follows on the basis of the incompressibility during the transition:

$$\Delta F = F'' - F' = (S_1' - S_1)\sigma_{10} + N S_2(\sigma_{20} - \sigma_{12}), \tag{4.3}$$

in which ρ_i, $V_i F_i (i = 0, 1, 2)$ are the densities, volumes, and free energies per unit mass respectively for the media (0), (1), and (2). With α_2 the volume concentration of the dispersed phase in s1, then the volume content of the liquid in the system is $1 - \alpha_2$. As the fragment in s1 and the liquid volume in s2 are spherical, we have on the basis that the liquid is incompressible and the relation between the volume V and surface S of a sphere $V = S^{3/2}/6\sqrt{\pi}$ that

$$S_1' = (1 - \alpha_2)^{2/3} S_1. \tag{4.4}$$

Now let V_1 be the liquid volume in the system and V_2 the volume of a spherical particle; then $\alpha_2 = NV_2/(NV_2 + V_1) = NS_2^{3/2}/(NS_2^{3/2} + S_1'^{3/2})$, and from (4.1) we have

$$N S_2 = S_1 \sqrt[3]{N\alpha_2^2}. \tag{4.5}$$

Finally, we substitute (4.4) and (4.5) into (4.3) and use the standard condition for the equilibrium in interfacial tension at the common boundary of the media (0), (1), and (2), $\sigma_{20} - \sigma_{12} = \sigma_{10}\cos\theta$ (θ is the wetting angle for the solid surface by the liquid) to get

$$\Delta F = S_1 \left\{ \sqrt[3]{N\alpha_2^2}\cos\theta - [1 - (1 - \alpha_2)^{2/3}] \right\} \sigma_{10}. \tag{4.6}$$

If $\Delta F > 0$, s1 is stable, since the transition to s2 is accompanied by an increase in the free energy; if $\Delta F < 0$, s1 is thermodynamically unstable.

From (4.6), the thermodynamic stability of the fragment structure is dependent on the volume and number concentrations of the particles, as well as on the angle θ characterizing the wettability of the particles by the given liquid.

Figure 5c shows a family of $\Delta F(\alpha_2, \theta, N = N_j) = 0$ curves constructed from (4.6). Each curve separates a region of stability $\Delta F(\alpha_2, \theta, N_j) > 0$ from a region of instability $\Delta F(\alpha_2, \theta, N_j) < 0$ in the s1 structure as functions of θ and α_2 for a given $N = N_j$. Under otherwise equal conditions, increase in N is a stabilizing factor for the s1 structure. For a given N_j, the structure is the more stable the higher the wettability (i.e., the less θ) and the lower α_2. If $\theta < 42°$, the s1 structure is thermodynamically stable for any $N_j \geq 1$ and $0 < \alpha_2 < \alpha_{2*} = 0.77$. If $\theta > 90°$, the s1 structure is unstable for any N_j and

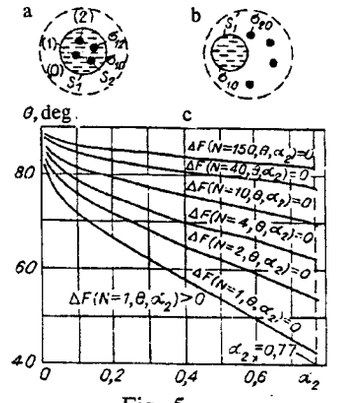

Fig. 5

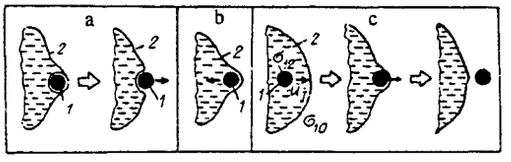

Fig. 6

$< \alpha_2 < \alpha_{2*}$. We can demonstrate this on an example where the solid particles are completely unwettable, i.e., $\theta = 180°$. Then s1 is the liquid matrix (1) located in the air medium (0) (Fig. 5a) and containing spherical particles (2), but with the surface S_2 of the particles separated from the liquid by thin air layers. We denote the volume of an air layer by ω_0 and the surface area at the liquid-air layer boundary by S_3. Then the total free energy of s1 is

$$F' = \rho_0 V_0 F_0 + \rho_1 V_1 F_1 + \rho_2 V_2 F_2 + N\rho_0\omega_0 F_0 + S_1\sigma_{10} + N(S_3\sigma_{10} + S_2\sigma_{20}). \tag{4.7}$$

The total free energy becomes as follows when s1 becomes s2 because of the separation between the liquid and solid phases:

$$F'' = \rho_0 V_0 F_0 + \rho_1 V_1 F_1 + \rho_2 V_2 F_2 + N\rho_0\omega_0 F_0 + S'_1\sigma_{10} + NS_2\sigma_{20}. \tag{4.8}$$

We subtract (4.7) from (4.8) to get

$$\Delta F = F'' - F' = -(S_1 + NS_3 - S'_1)\sigma_{10}. \tag{4.9}$$

Then as $S_1 > S_1'$ for any $\Delta F < 0$ and $N \geq 1$, i.e., s1 is thermodynamically unstable, since on transition to s2, the total free surface is reduced by NS_3, so the free energy is reduced by $NS_3\sigma_{20}$.

This thermodynamic stability analysis involves the assumption that the particles are frozen in the liquid, so one can separate the liquid and solid phases only by deforming the volume of the suspension, in which particle 1 (Fig. 6a, b) is near the free surface 2 and is repelled by capillary forces into the atmosphere (lyophobic case, Fig. 6a) or return from the free surface into the liquid volume (lyophilic case, Fig. 6b).

However, $\rho_1 \neq \rho_2$ in almost any suspension, so in a real failure process, the particle may be displaced with respect to the liquid at some velocity u_j. Then the structure stability is dependent on the ratio between the kinetic energy of the particle E_j and the difference in the surface energies in the liquid and the atmosphere, i.e., the condition for emergence of particle 1 of radius r_j from volume 2 (Fig. 6c) is written as follows without allowance for the viscous losses:

$$E_j = \frac{2}{3}\pi r_j^3 \rho_2 u_j^2 > F_{20} - F_{12} = 4\pi r_j^2 \sigma_{10}\cos\theta, \tag{4.10}$$

in which $F_{12} = 4\pi r_j^2\sigma_{12}$ and $F_{20} = 4\pi r_j^2\sigma_{20}$ are the surface energies of a spherical particle in the liquid and after emergence into the atmosphere respectively; $\theta \leq 90°$, since $E_j > F_{20} - F_{12}$ for any u_j for $\theta > 90°$. It follows from (4.10) that if u_j satisfies

$$u_j > \sqrt{\frac{6\sigma_{10}}{r_j \rho_2} \cos\theta} \quad \text{for} \quad \theta \leq 90°, \tag{4.11}$$

the particle will overcome the surface elasticity and escapes into the atmosphere, while if (4.11) is not obeyed, the capillary forces return the particle to the liquid.

In the lyophilic C2 medium, C2 $\theta < 10°$, $\rho_2 \simeq 2.6$ g/cm^3, and $r_j \leq 0.005$ cm, $\sigma_{10} = 72.3$ g/sec^2, and from (4.11) the particle will emerge from the liquid into the atmosphere if $u_j > 1.8$ m/sec, which is unrealistic because the rate of increase in the linear dimensions of the medium during stretching in the experiments did not exceed 3-4 m/sec. Then the structure ofC2 is preserved during the fragmention: the phases do not separate. On the other hand $\theta > 90°$ for C4, and (4.6) and (4.9) imply that the structure is unstable even if the particles are frozen in ($u_j = 0$). The research was performed with financial support from the Russian Fundamental Research Fund in accordance with project 93-013-16383.

REFERENCES

1. Lubowitz (ed.), Failure [Russian translation], Mir, Moscow (1973)-(1976), Vols. 1-7.
2. A. N. Dremin, G. I. Kanel', and S. A. Koldunov, "A study of spalling in water, ethyl alcohol, and plexiglas," in: Combustion and Explosion: Proc. 3rd All-Union Symposium on Combustion and Explosion [in Russian], Nauka, Moscow (1972).
3. G. A. Carlson and K. W. Henry, "Technique for studying tensile failure in application to glycerol," J. Appl. Phys., **44**, No. 5 (1973).
4. V. K. Kedrinskii, "The experimental research and hydrodynamical models of a "sultan," Arch. Mech., **26**, No. 3 (1974).
5. S. V. Stebnovskii, "The mechanism of pulsed failure in a liquid volume," Prikl. Mekh. Tekhn. Fiz., No. 2 (1989).
6. S. V. Stebnovskii, "Shear elasticity in a liquid medium containing bubbles," Fiz. Gor. Vzryva, No. 3 (1990).
7. S. V. Stebnovskii, "Instability in bubble structures in a liquid medium," in: Continuous-Medium Dynamics [in Russian], Coll., Inst. Gidrodinamiki, Sib. Otd. AN Akad. Nauk SSSR (1991).
8. R. Pal and E. Rhodes, "Viscosity Concentration relationship for emulsion," J. Rheol., **33**, No. 7 (1989).
9. L. Nilsen, Mechanical Properties of Polymers and Polymer Composites [Russian translation], Khimiya, Moscow (1978).
10. M. Cornfeld, Elasticity and Strength in Liquids [Russian translation], GITTL, Moscow–Leningrad (1951).
11. V. E. Dontsov, V. V. Kuznetsov, and V. E. Nakoryakov, "Pressure-wave propagation in a porous medium saturated with liquid," Prikl. Mekh. Tekhn. Fiz., No. 1 (1988).
12. I. R. Baikov, A. R. Berngardt, V. K. Kedrinskii, and E. I. Pal'chikov, "Experimental methods of examining the dynamics of cavitational clusters," Prikl. Mekh. Tekhn. Fiz., No. 5 (1984).
13. S. V. Stebnovskii, "Formation dynamics of a gas-droplet flow in explosive dispersal of a liquid volume," in: Dynamics of Continuous Media [in Russian], Coll., Inst. Gidrodinamiki, Sib. Otd. RAN (1992).